Journal of GeoEngineering, Vol. 9, No. 3, pp. 85-93, December 2014
http://dx.doi.org/10.6310/jog.2014.9(3).1

A *p-y* CURVE-BASED APPROACH TO ANALYZE PILE BEHAVIOR IN LIQUEFIED SAND UNDER DIFFERENT STRESS STATES

Sheng-Huoo Ni[1], Xiong Xiao[2], and Yu-Zhang Yang[2]

ABSTRACT

In general, *p-y* curves that represent the soil resisting force per unit length of pile as a function of soil displacement are used to model the interaction behavior of soil and pile. However, there are significant uncertainties about how to model soil-pile behavior in liquefied sand, especially for the different softening effect of liquefied soil under different states of soil-pile interaction. A new *p-y* model, which is capable of reflecting the dilative behavior of soil and the gap effect under different soil stress states, is presented in an attempt to develop a practical approach for soil-pile interaction behavior. This *p-y* model incorporates an upper-bound *p-y* curve calculated from the improved *p*-multiplier and *y*-multiplier and a lower-bound *p-y* curve regarding the residual state of the soil-pile reaction in liquefied sand. Also, for the stress state between the two boundaries, the *p-y* curve can be approximately obtained from linear interpolation. The comparison between calculated results and the results of pile lateral-load test, which was taken in medium dense sand liquefied by blast load, indicate that the proposed *p-y* model provides reasonable estimates of response for piles in liquefied medium dense sand while pile-head displacements were less than 150 mm.

Key words: Piles, soil liquefaction, soil-pile response, lateral loads, stress state.

1. INTRODUCTION

Soil liquefaction induced by earthquakes and other cyclic loading is one of the major causes of damage to pile structures. However, the prediction of soil-pile responses in liquefied sand is quite complex. Some studies have been conducted to account for that load-resistance behavior. Liu and Dobry (1995) performed a group of centrifuge tests to study pile behavior in sand with certain levels of excess pore pressure. A series of reduction factors (*i.e. p*-multipliers) was therefore recommended to compensate for this softening effect on sand approaching liquefaction and a *p*-multiplier of 0.1 was suggested for liquefied sand. Wilson (1998) and Wilson *et al.* (2000) also proposed back-calculated *p*-multipliers ranging from 0.1 to 0.35 based on the initial relative density of liquefied sand. Tokimatsu (1999) observed that the field performance of piles subjected to lateral spreading was strongly related to the safety against liquefaction (F_L) factor, and *p*-multipliers ranging from 0.05 to 0.2 were suggested. However, the results in this paper showed that it is not sufficient to consider this problem without adding a *y*-factor. Wang and Reese (1998) incorporated the use of *p-y* relationships for soft clay (Matlock 1970) based on the undrained residual strength (S_r) of sand to account for the reduced resistance provided by liquefied sand. S_r is commonly estimated from its relationship related to $(N_1)_{60}$ (Seed and Harder 1990). Gillette (2010) showed that the S_r suggested by Seed and Harder (1990) may not fit well with the observed soil resistance of near-surface soils which provide the main resistance to laterally loaded pile. This means Wang and Reese's method had a built in limitation to account for the effect of confining pressures. Weaver *et al.* (2005) gave a comparison between the estimation of soil-pile behavior using a *p-y* curve modified according to the above recommendations and full-scale test data. The results demonstrated that these simple methods tend to over-predict the soil resistance at small displacements and do not reflect the dilative behavior often observed during the shearing of medium-dense sand. Rollins *et al.* (2005) developed an empirical *p-y* curve to quantify the dilative behavior of liquefied sand. Ashour and Ardalan (2012) proposed the strain wedge model to assess the *p-y* curve for piles in fully liquefied saturated sands by using a liquefied sand stress-strain model. This method requires a complicated iteration process and the accuracy of this technique is influenced by the method used to estimate the soil properties. Dash *et al*. (2008) reviewed the most commonly used models for the *p-y* curve for liquefied soils, and subsequently, a group of *p-y* curves were presented for the sandy soil transit from a non-liquefied state to a fully liquefied state characterized by an excess pore pressure ratio. Also, some studies (*e.g.*, Ishihara and Cubrinovski 2004; JRA 1996; Tokimatsu 2003; Lin *et al*. 2005; Chang *et al*. 2008) had already discussed the situation of liquefaction-caused lateral spreading with the consideration of ground motion induced earth pressure in piles. However, the mechanism in the research referenced above was different from the one discussed in this paper.

This paper focused on the performance of the proposed *p-y* curve-based procedure to evaluate pile behavior in level-ground liquefied sand. As shown in this study, it is impossible to simulate the soil-pile interaction of different load states using a single *p-y* curve. The full-scale test results, which represented the initial load state, medium load state and residual load state of soil-pile reaction in liquefied sand, provided by Ashford and Rollins (2002), were compared to results from the analyses which implement *p-y* curves modified by *p*-multipliers and *y*-multipliers, interpolated *p-y* curves and Rollins' *p-y* curves, respectively. This overall process of lateral-load test was taken place in sand after

Manuscript received June 10, 2014; revised October 14, 2014; accepted October 20, 2014.
[1] Professor (corresponding author), Department of Civil Engineering, National Cheng Kung University, Taiwan (e-mail: tonyni@mail.ncku.edu.tw).
[2] Graduate Student, Department of Civil Engineering, National Cheng Kung University, Taiwan.

blast induced liquefaction, and initial state indicates the condition of no relative lateral displacement had yet occurred between soil and pile; residual state indicates the condition which the curve of load *vs*. displacement remain the same while the number of load cycle increased and with a 50 mm relative lateral displacement between soil and pile; medium state indicates the condition of relative lateral displacement between above two conditions.

2. THEORETICAL BACKGROUND

2.1 Excess Pore Water Pressure Response

Previous work of Dobry and Abdoun (1998), Kutter and Wilson (1999) and Tokimatsu *et al.* (2005) suggested that during phase transformation, a sudden drop in excess pore pressure will cause the resistance to pile displacement in medium-dense liquefied sands to increase. The observance of this dilative behavior in response to pile movement is important in verifying models used to predict soil-pile interaction in liquefied sands. A detailed review of the relationship between excess pore water pressure and applied load is able to provide information that explains this dilative behavior and reveals soil behavior in response to lateral loaded piles in liquefied sand.

The measured pore water pressure near a 0.6 m cast-in-steel-shell (CISS) pile presented by Ashford and Rollins (2002) explains this dilative behavior, as shown in Fig. 1. Excess pore water pressure ratio near the pile shows a small initial increase in excess pore pressure as the pile is pushed toward the piezometer. However, it can be seen that as the pile continues to displaced, the excess pore water pressure begins to reduce until the maximum pile displacement is reached. The reduction in excess pore water pressure indicates that liquefied soils may provide significant resistance to pile movement as a result of a phase transformation. As the pile is unloaded, excess pore water pressure begins to increase initially but decreases as the pile continues to unload. It can be seen that dilative behavior was not noticeable at 4.2 m from the center of the 0.6 m CISS pile or at greater depths (Fig. 1).

Therefore, while analyzing soil-pile reactions in liquefied sand, one must consider the ascension of soil stiffness induced by this phase transformation. A concave-up shape *p-y* curve is needed.

2.2 Gap Effect

A gap was formed between the pile and the soil when several cycles of shaking force were conducted during the full-scale tests, which is partially responsible for the generation of zero resistance zones. The plot of load versus displacement of the 0.6 m CISS pile (Fig. 2) for the first post-blast series shows that the gap generation increased with load cycle, and was able to yield a 50 mm gap after the 9th cycle with maximum displacements of 228 mm. With the pile displacement increased, the soil can make contact with the pile body again, and soil stiffness is recovered in this stage. The soil-pile response predicted by the use of standard sand *p-y* curves (Reese *et al.* 1974), which have a high initial soil resistance slope, contradicted the phenomena of zero resistance and soil stiffness recovery. Therefore, a gap effect is another possible reason for a concave-up shaped *p-y* curve.

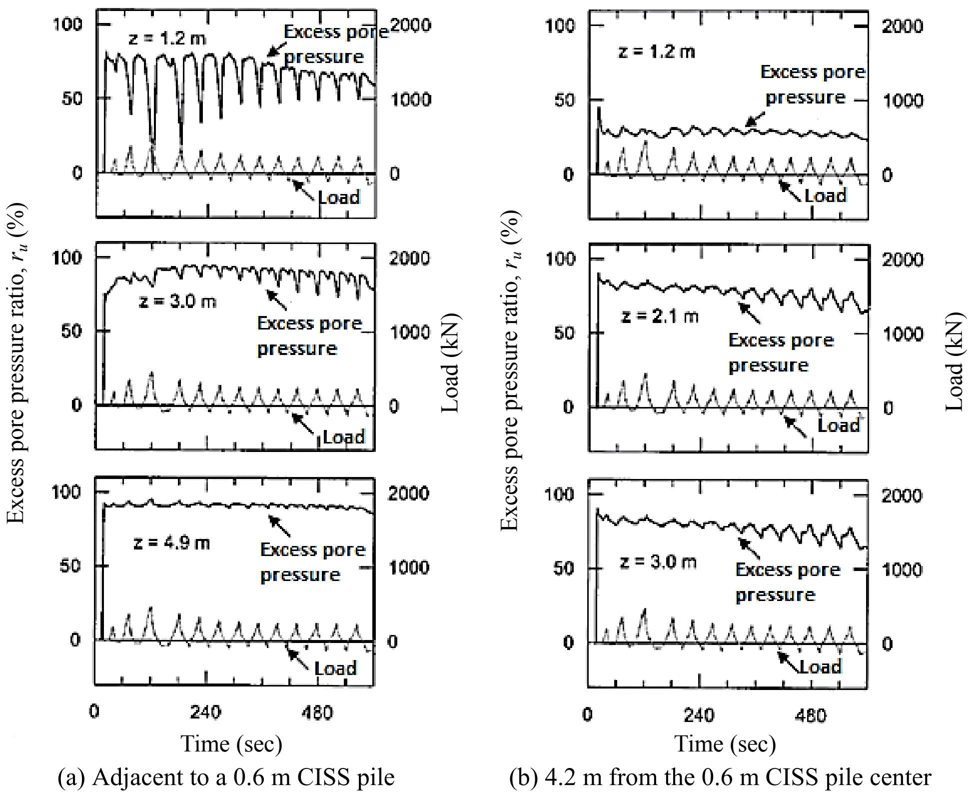

Fig. 1 Excess pore water pressure ratio and load versus time (Ashford and Rollins 2002)

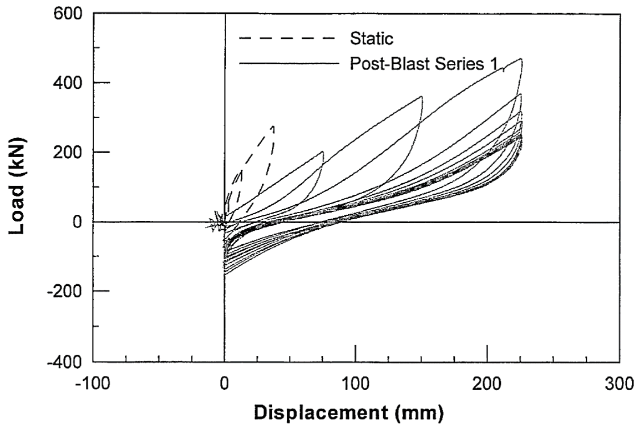

Fig. 2 Load versus displacement of the 0.6 m CISS pile for the first post-blast series (Ashford and Rollins 2002)

2.3 A *p-y* Curve-based Procedure to Analyze Pile Behavior in Liquefied Sand

Different soil-pile interactions were observed in different stress states as the excess pore water pressure was generated. As shown in Fig. 2, the softening effect of the soil for the first cycle, with a maximum pile head displacement of 73 mm, is not as significant as that exhibited in the 9th cycle, with a maximum pile head displacement of 228 mm. Therefore, the dilative and gap effect became more obvious as more load cycles were conducted to displace the pile. A new procedure for analyzing pile behavior in liquefied sand is described as follows:

1. When the pile was surrounded by liquefied soil with certain levels of excess pore pressure generated, and no gap was formed between them, soil stiffness was mainly affected by the drop in effective soil stress. For this case, an upper bound *p-y* curve should be given to simulate the pile behavior.
2. With the load cycle number is increased, there will be gaps generated between the soil and pile. As the gaps grow to their maximum widths, and excess pore pressure is maintain at a relatively higher level (80% or higher), the decrease in soil stiffness is no longer due only to the effective stress drop, but is also caused by the generation of a zero resistance zone. Therefore, a lower bound *p-y* curve should be used to model this residual soil-pile response state.
3. For states between the above two cases, linear interpolated *p-y* curves can be used to account for this medium soil-pile interaction state.

A. Upper bound *p-y* curves for liquefied sand

Under conditions in which soil is not being separated from the pile body, a *p-y* curve (Reese *et al.* 1974) modified by a *p*-multiplier and a *y*-multiplier can be used to model the soil-pile reaction. The *p*-multiplier suggested by Liu and Dobry (1995) is recommended.

Liu and Dobry (1995) performed a group of centrifuge tests to quantify excess pore water pressure's effect on the lateral load capacity of steel pile in liquefied sand. The scaling factor of the centrifuge test was 40. The prototype steel pile was 6.7 m long, 0.381 m in the outside diameter, 0.353 m in the inside diameter, with a bending stiffness of $EI = 5241.7$ kN·m^2. A series of cyclic lateral forces F_0 was conducted to cause a maximum pile head displacement of 5 cm at 5 seconds after shaking, while a certain level of excess pore water pressure was generated. In this case, when the pore water pressure was large, less force was needed to displace the pile to 5 cm. The degradation rate of soil resistance for certain pore water pressure ratios is back-calculated and shown in Fig. 3 below. In this plot, dimensionless degradation parameter K_u is more or less uniquely correlated with r_u. This relationship has been suggested to establish the effect of excess pore water pressure in the sand on *p-y* curves at different depths along the pile (the *p*-multiplier). The effect of the *y*-multiplier will be discussed in the program LPILE modeling below.

B. Lower bound *p-y* curves for liquefied sand

Based on the results of Ashford and Rollins's (2002) full-scale pile tests, Rollins *et al.* (2005) developed an empirical mathematical equation to describe the concave-up soil-pile response in liquefied sand. This mathematical model is back-calculated from the 10th load cycle. As shown in Fig. 2, the initial soil resistance of each load cycle decreases during shearing until the 10th load cycle, at which time this initial soil resistance will be kept constant, which means a residual phase of the soil-pile response is reached. The mathematical expression for this residual phase is shown as Eq. (1):

$$p = A(By)^C(p_d) \tag{1}$$

where $A = 3 \times 10^{-7}(z+1)^{6.05}$
$B = 2.80\,(z+1)^{0.11}$
$C = 2.85\,(z+1)^{-0.41}$
$P_d = 3.81\,(\ln d) + 5.6$

where p is the soil pressure per unit length of the pile (kN/m); y is the relative differential displacement between pile and soil (mm); z is the depth of interest from the ground surface (m); P_d is the diameter adjustment factor; and d is the diameter of the pile (m).

Equation (1) should generally be used in conditions similar to those of the full-scale test, namely for soil pressures of 55 kN/m or less, deflections of 150 mm or less, and sands with relative densities of approximately 50%.

C. Linear interpolation of *p-y* curves

For the soil stress state between the two boundaries, the *p-y* curve can be approximately obtained from linear interpolation. Taking the 3rd load cycle as an example, which is located in the middle of the 1st and 9th load cycle, the soil-pile response of this intermediary state is modeled by averaging the *p-y* curves of the upper and lower boundaries.

The three *p-y* curves discussed above in the theoretical background section are shown in Fig. 4. The standard Reese sand *p-y* curve (Reese *et al.* 1974) was given to provide a comparison with these three *p-y* curves.

3. CASE STUDY

3.1 Overview of the Full-Scale Field Test

Ashford *et al.* (2002) conducted a group of full-scale pile tests on Treasure Island in San Francisco, California to study the lateral load behavior of piles in liquefied soil. In their tests, pile head displacements and lateral loads were measured by potentiometer and load cells, separately. Piezometers were installed along pile and at a radial distance of approximately 4.2 m from the pile center to measure the excess pore water pressure. Liquefaction was induced by detonating down-hole explosives. A high speed hydraulic actuator was used to apply half-cyclic lateral loading to the 0.6 m and 0.9 m CISS pile. The series of loading cycles for the 0.6 m CISS pile consisted of one 73 mm, one 150 mm, and ten 228 mm displacements and ten 36 mm, one 76 mm, one 152 mm and eleven 225 mm displacements for the 0.9 m CISS pile.

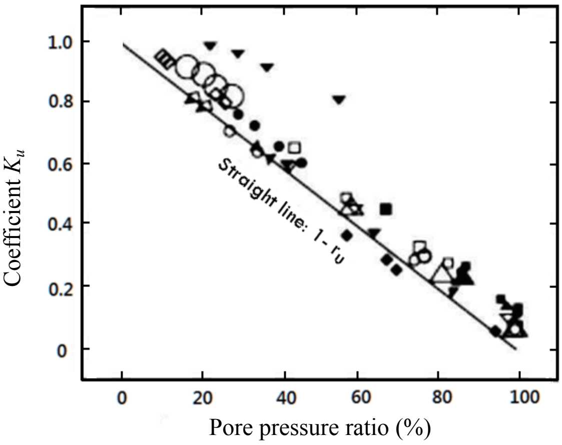

Fig. 3 Excess Pore water Pressure Ratio r_u versus degradation parameter K_u (Liu and Dobry 1995)

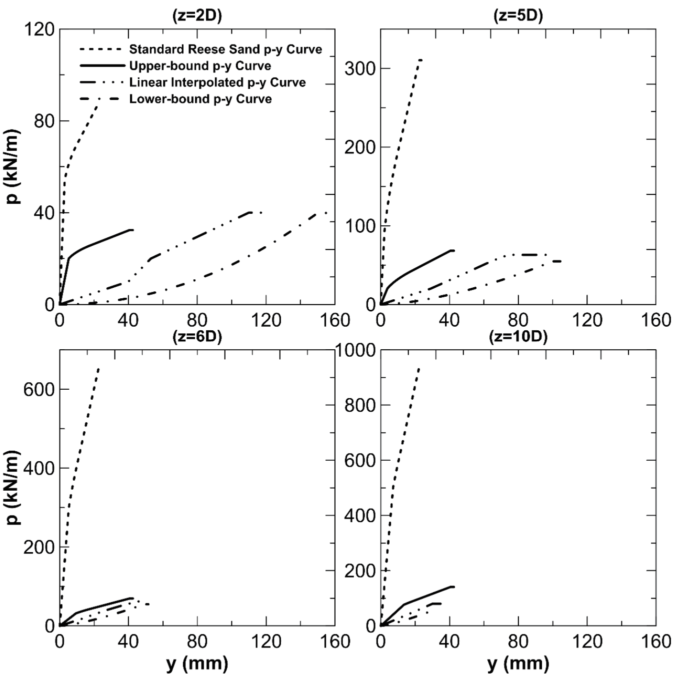

Fig. 4 Comparison between the proposed *p-y* curves and the Reese sand *p-y* curve

3.2 Soil and Pile Property

The full-scale pile lateral load tests were performed at Treasure Island's National Geotechnical Experimentation Site, where well-documented investigations have been previously conducted, including the results of the Standard Penetration Test (SPT) and Cone Penetration Test (CPT). Relative density (D_r) can be estimated according to the empirical relationship between SPT-N value with D_r as proposed by Kulhawy and Mayne (1990), and the D_r for the sand layers in this case are approximately 50%. The horizontal subgrade reaction (k), friction angle (ϕ), and total unit weight (γ) were obtained using a relationship with D_r proposed by the American Petroleum Institute (API 2005). The total unit weight value was assumed for each of the layers: 19.5 kN/m^3 for sand above the water table, 21.1 kN/m^3 for sand below the water table, 9.5 kN/m^3 for grey clay, and the soil properties used in the lateral pile analysis are shown in Table 1 and Table 2 below. The pile properties are shown in Table 3 below.

Table 1 Soil layering and properties used in lateral pile analysis for 0.6 m CISS pile

Depth below excavated ground		Type of soil	Effective unit weight (kN/m^3)	Cohesion c (kPa)	Friction Angle ϕ (°)	Lateral Subgrade Modulus, k (MN/m^3)	ε_{50}
Top (m)	Bottom (m)						
0	0.51	sand	19.5	0	33	24.4	–
0.51	2.59	sand	11.1	0	33	15.4	–
2.59	4.73	sand	11.1	0	32	13.6	–
4.73	7.49	sand	11.1	0	30	10.8	–
7.49	9.25	soft clay	9.5	19.2	0	–	0.01
9.25	10.16	sand	11.1	0	30	10.8	–
10.16	17.8	soft clay	9.5	19.2	0	–	0.01

Table 2 Soil layering and properties used in lateral pile analysis for 0.9 m CISS pile

Depth below excavated ground		Type of soil	Effective unit weight (kN/m^3)	Cohesion c (kPa)	Friction Angle ϕ (°)	Lateral Subgrade Modulus, k (MN/m^3)	ε_{50}
Top (m)	Bottom (m)						
0	1.6	sand	19.5	0	33	24.4	—
1.6	6	sand	11.1	0	33	15.4	—
6	8.1	sand	11.1	0	30	10.8	—
8.1	9.9	soft clay	9.5	19.2	0	—	0.01
9.9	13.1	sand	11.1	0	30	10.8	—
13.1	24.4	soft clay	9.5	19.2	0	—	0.01

Table 3 Properties of CISS pile

Length (m)	Outside diameter (m)	Bending stiffness EI (kN/m^2)
13.9	0.6	291800
12	0.9	1019358

3.3 Numerical Modeling

In this study, a finite difference method computer program, LPILE 2013 V.7 (Isenhower and Wang 2013) was used to predict the pile displacements. LPILE 2013 is a widely used program for analyzing a pile under lateral loading developed by ENSOFT, Inc., Austin, Texas. Soil behavior is modeled with *p-y* curves internally generated by the computer program following published recommendations for various types of soils or with *p-y* curves manually introduced by the user.

To verify the procedures presented in this paper, the *p-y* curves mentioned in the previous section were exported into the LPILE 2013 program to simulate the soil-pile response in liquefied sand. The calculation procedures are given as follows:

1. The calculated soil-pile reactions using the upper-bound *p-y* curve were compared with the full-scale test result for the 1st load cycle of the 0.6 m CISS pile and the 1st load cycle of the 0.9 m CISS pile.
2. The residual soil-pile reaction states calculated by the lower-bound *p-y* curve were compared with the full-scale test result of the 9th load cycle of the 0.6 m CISS pile and the 19th load cycle of the 0.9 m CISS pile.
3. For the load cycle between the above two cases, the linear Interpolated *p-y* curve was used to model the soil-pile reaction. In this paper, the test results for the 3rd load cycle of the 0.6 m CISS pile and the 12th load cycle of the 0.9 m CISS pile, located in the middle of the upper and lower bound, were compared to the calculated results of the averaged *p-y* curve. This *p-y* curve is the average of the upper and lower bound *p-y* curves.

In addition, the percentage error between the calculated displacement and the full-scale test result is defined as Eq. (2).

$$\text{error}(\%) = \frac{D_{\text{calculated}} - D_{\text{measured}}}{D_{\text{measured}}} \tag{2}$$

where $D_{\text{calculated}}$ and D_{measured} are the calculated and measured pile head displacements, respectively.

4. Results and Discussion

4.1 Calculation of 0.6 m CISS Pile

A. 1st load cycle with a maximum pile head displacement of 73 mm

In this case, firstly, only *p*-multipliers were used to modify *p-y* curve, and the dilative effect was not considered. The comparison between the results for the actual measured value and calculated results are shown in Fig. 5. The values of the *p*-multipliers are related to the excess pore water pressure at different depths, which were measured when no lateral loads were applied at the pile top, following Liu and Dobry's (1995) suggestion. The *p-y* curves modified in this way were then used to model the 0.6 m CISS pile behavior in the 1st load cycle. Since this modified method has been suggested by many previous practitioners, for convenience, this procedure is called the traditional method (Fig. 5). Under a small lateral load, the calculated pile-head displacements converge with the test results, for which the error percentage is below 5%. However, it can be seen that as the lateral load increased, the error percentage grew as well. A lateral

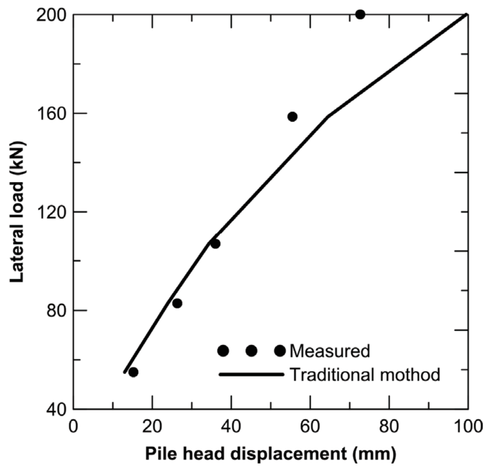

Fig. 5 Load versus pile head displacement for the 0.6 m CISS pile in the 1st load cycle

load of 200 kN produces an error percentage of 37%. It appears the error will become larger at larger displacements based on a comparison of the slopes of the load-displacement curves. The error is produced because the dilation of sand in the large pile head displacement in the modified method is not considered.

Then, the upper-bound *p-y* curves presented in this paper are used to model pile behavior for the same case. In order to quantify the dilative effect properly, the pore water pressure values for each lateral load (shown in Fig. 6) are used to modify the soil resistance by using *p*-value). The calculation results for the pile head displacements for each lateral load are shown in Fig. 7. If we considered only the dilative effect with no multiplying a *y*-factor to *p-y* curves, the calculated results are smaller than the test results with a maximum error of 21% at a lateral load of 200 kN. If the lateral displacement is multiplied by a *y*-factor of 1.8, the calculated results agree well with the test results, which means both *p*-multipliers and *y*-multipliers should be given to model the softening of the soil-pile response for pore water pressure building up during an earthquake in a liquefied sand deposit.

B. 9th load cycle with a maximum pile head displacement of 228 mm

In this case, lower-bound *p-y* curves (Rollins *et al.* 2005) were used to model the soil-pile reaction of the 0.6 m CISS pile in its 9th load cycle. The results are shown in Fig. 8. Except for the maximum 12.3% error at a lateral load of 255 kN, the calculated results match the test results. This error is possibly caused by the limitation of the Rollins' model, which only allows an ultimate soil resistance of 55 kPa and a maximum pile head displacement of 150 mm. Also, as shown in Fig. 9, the moment curves that calculated using lower-bound *p-y* curves matched well with the field measured moments along the pile.

C. 3rd load cycle with a maximum pile head displacement of 228 mm

In the case of the medium stress state, the 3rd load cycle, upper-bound *p-y* curves were first given to model the soil-pile interaction. The pore water pressure values for each lateral load are shown in Fig. 10. The calculated pile head displacements for each lateral load are shown in Fig. 11. If a *y*-multiplier of 3.8 is

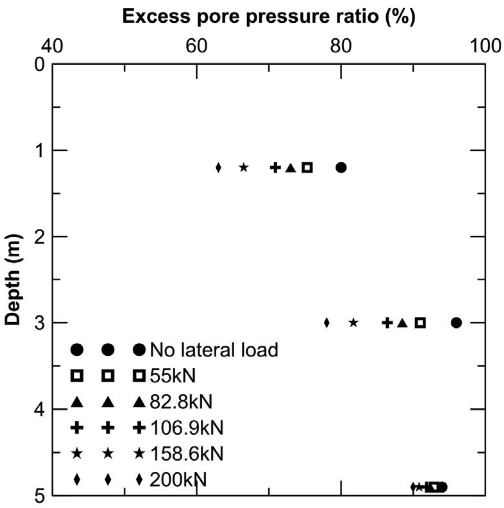

Fig. 6 Excess pore pressure ratio for 0.6 m CISS pile in the 1st load cycle

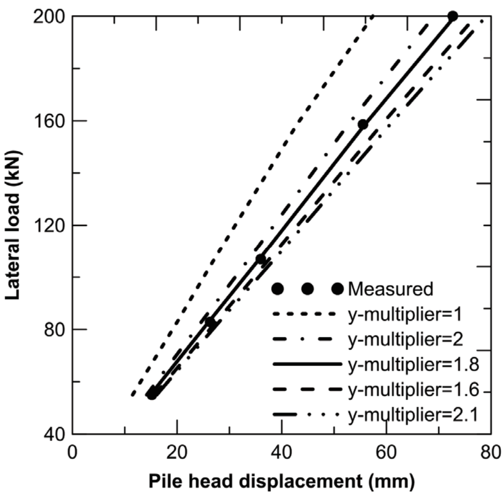

Fig. 7 Load versus pile head displacement for 0.6 m CISS pile in the 1st load cycle (using upper-bound *p-y* curve)

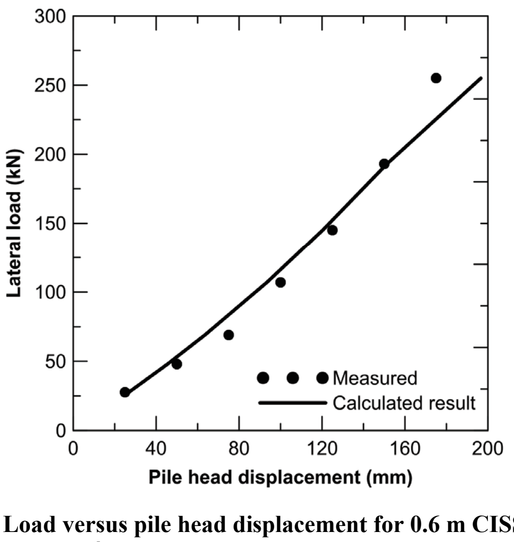

Fig. 8 Load versus pile head displacement for 0.6 m CISS pile in the 10th load cycle

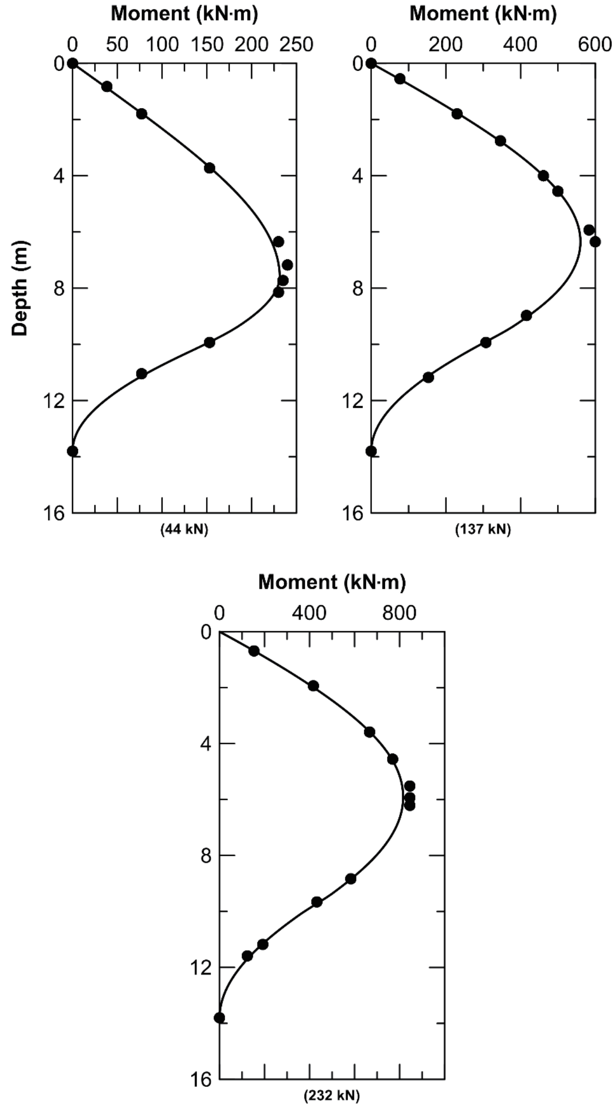

Fig. 9 Comparison of analyses using lower-bound *p-y* curve with measured moment

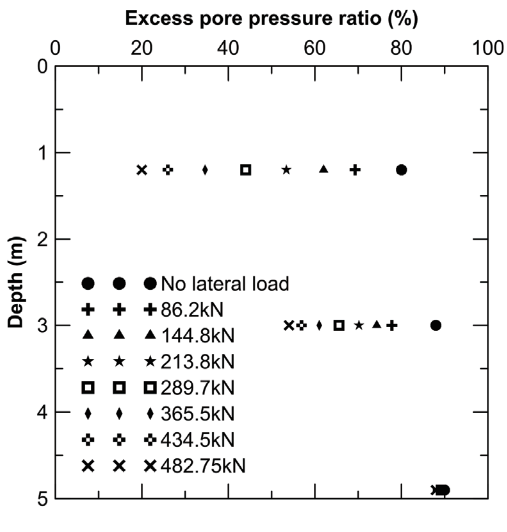

Fig. 10 Excess pore water pressure ratio for 0.6 m CISS pile in the 3rd load cycle

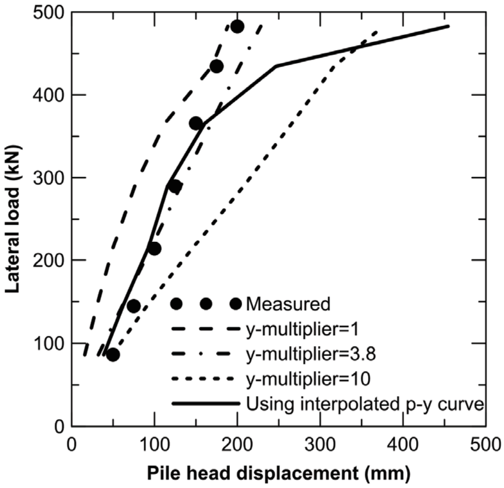

Fig. 11 Load versus pile head displacement for 0.6 m CISS pile in the 3rd load cycle

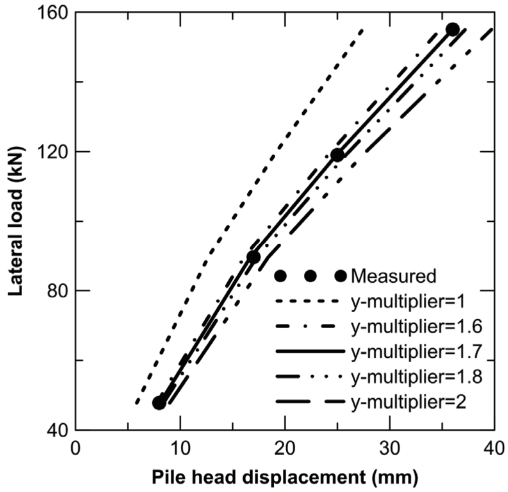

Fig. 12 Load versus pile head displacement for the 0.9 m CISS pile in the 1st load cycle

used, errors in the results between calculated and measured results are acceptable, with the highest error of 35.6% at a lateral load of 86.2 kN. The linear interpolation *p-y* curves as presented in this paper are conducted to model the same case. When the lateral load is less than 350 kN, and the pile head displacement is less than 150 mm, the calculated results agree well with the measured data, and the error at a lateral load of 86.2 kN is reduced to 20%. However, due to the limitations of the model in regard to ultimate soil resistance and maximum pile head displacement, this method is unable to simulate the situation of a large lateral load. Therefore, the method using average *p-y* curves can predict the soil-pile response for the medium stress state case better than the method using an upper-bound *p-y* curve.

4.2 Calculation for the 0.9 m CISS Pile

A. 1st load cycle with a maximum pile head displacement of 36 mm

The new simplified method, as proposed in the 0.6 m CISS pile case, using *p*-multipliers and *y*-multipliers, was given to model the 0.9 m CISS pile behavior in the 1st load cycle with a maximum pile head displacement of 36 mm. The excess water pore pressure at different depths is kept at 90% or higher during the loading cyclic to maintain the *p*-multiplier at 0.1. As shown in Fig. 12, the calculated results of soil-pile response using this simplified method agree well with the test results with a *y*-multiplier of 1.7.

B. 19th load cycle with a maximum pile head displacement of 225 mm

The test results for the 0.9 m CISS pile shows that the soil pile system decreased in stiffness during the first 18 cycles and that the decrease in stiffness for the final six 225 mm cycles was negligible. A Rollins' *p-y* curve was conducted to model this residual soil-pile reaction. The results are shown in Fig. 13. The same as the 0.6 m CISS pile case, the calculated results match the test results except for the maximum158.3% error at a lateral load of 489.6 kN. This error was possibly caused by the limitation of the Rollins' model, which only allows an ultimate soil resistance of 78 kPa and a maximum pile head displacement of 150 mm.

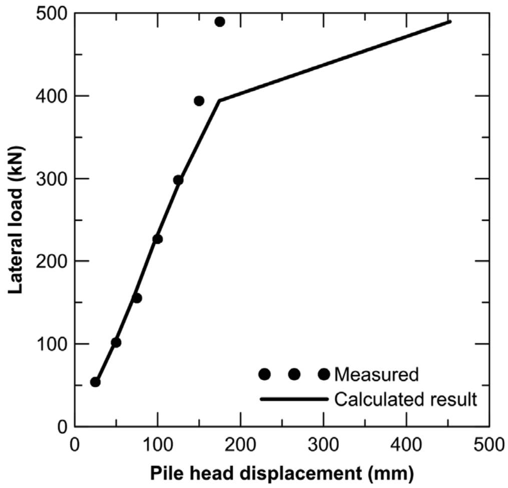

Fig. 13 Load versus pile head displacement for 0.9 m CISS pile in the 19th load cycle

C. 12th load cycle with a maximum pile head displacement of 225 mm

The *p-y* curves, which were obtained by averaging the *p-y* curves of the 1st and 19th cycles, were conducted to model the stress state case between the two boundaries. Figure 14 illustrates that while the lateral load is less than 585 kN, and the pile head displacement is less than 150 mm, the calculated results agree well with the test data. However, due to the limitation of the model in regard to ultimate soil resistance and maximum pile head displacement, this method cannot be used to simulate a large lateral load situation.

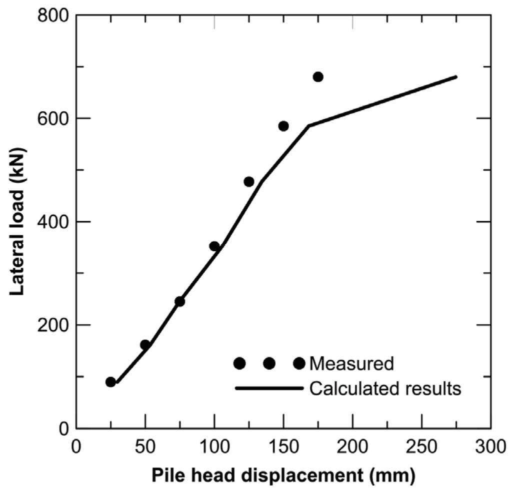

Fig. 14 Load versus pile head displacement for the 0.9 m CISS pile in the 12th load cycle

5. CONCLUSION REMARKS

The soil-pile response analyses performed using the *p-y* curves mentioned in this paper are confirmed for use to simulate pile behavior in liquefied sand under different stress state conditions. The results can provide practitioners a better understanding of how much resistance can be expected during liquefaction. However, this *p-y* model was applicable in sand liquefied by blast load, whether it is suitable for case of analyzing pile behavior in sand liquefied by seismic ground motion or not still need more study. The summarized findings and suggestions from this study are given as follows:

1. Dilative behaviors of soil and gap effects are the two main causes for different softening effects on a wide range of soil stress states. Ignoring this phase transformation will generally overestimate soil stiffness at small lateral pile displacements but will tend to underestimate soil stiffness for case where piles are displaced by large lateral loads. In order to properly use the upper-bound *p-y* curve, further study about the relationships between the change of excess pore pressure and the increased pile displacement were recommended.
2. Under the condition where no gap was generated around the pile in liquefied sand, and few load cycles were conducted to displace the pile, a simplified method with an upper-bound *p-y* curve can be used to account for the degradation in soil resistance. The *y*-multiplier is 1.8 for the 0.6 m CISS pile and 1.7 for the 0.9 m CISS pile in this study. More full-scale lateral pile load tests are needed to provide a database of information sufficient enough to determine the magnitude of *y*-multipliers for different piles.
3. When a residual phase of soil-pile response is reached, lower-bound *p-y* curves can be used to model the soil-pile reaction with restrictions of soil resistance less than 55 kPa; pile head displacement less than 150 mm and sand relative density approximately 50%.
4. For the soil stress state between these two boundaries, the linear interpolation *p-y* curve can be used to simulate the soil-pile response. The calculated results agree well with the test data except for the condition of the pile head displacement over the model restriction of 150 mm.
5. The choice of which curve to be used depends on the relative displacement between soil and pile while no lateral force was loaded on pile. When analyzing the behavior of 0.6 ~ 0.9 m CISS pile in medium dense sand liquefied by blast load, an upper bond *p-y* curve is suggested when there is no relative displacement between soil and pile; the lower bound *p-y* curve is suggested when the relative displacement between soil and pile reached 50 mm; in order to simplify the interpolation procedure, a linear interpolation is suggested when the relative displacement is between 0 and 50 mm. More pile load tests are warranted to provide a database of information sufficient enough to determine the relationship between relative pile displacement and the choice of *p-y* curve.

ACKNOWLEDGEMENTS

The study on which this paper is based was supported in part by the Ministry of Science and Technology, Taiwan, R.O.C. under grant number MOST 103-3113-E-006-004. Grateful appreciation is expressed for this support.

REFERENCES

American Petroleum Institute (API) (2005). *Recommended Practice for Planning, Designing, and Constructing Fixed Offshore Platform*, API Report No. 2A-WSD, API, Houston, Texas.

Ashford, S.A. and Rollins, K.M. (2002). *TILT: The Treasure Island Liquefaction Test: Final Report*, Report No. SSRR-2001/17, Department of Structural Engineering, Unversity of California at San Diego, California.

Ashour, M. and Ardalan, H. (2012). "*p-y* curve and lateral response of piles in fully liquefied sands." *Canadian Geotechnical Journal*, **49**(6), 633–650.

Chang, D.W., Lin, B.S., Yeh, C.H., and Cheng, S.H. (2008). "FD solutions for static and dynamic Winkler models with lateral spread induced earth pressures on piles." *Geotechnical Earthquake Engineering and Soil Dynamics IV*, **2**, 835−844.

Dash, S.R., Bhattacharya, S., Blakeborough, A., and Hyodo, M. (2008). "*p-y* curve to model lateral response of pile foundation in liquefied soils." *Proceedings of the 14th World Conference on Earthquake Engineering*, October 12-17, 2008, Beijing, China.

Dobry, R. and Abdoun, T. (1998). "Post-triggering response of liquefied sand in the free field and near foundations." *Proceedings of Geotechnical Earthquake Engineering and Soil Dynamics III*, Seattle, WA, *Geotechnical Special Publication*, ASCE, No. **75**(2), 270–300.

Gillette, D.R. (2010). "On the use of empirical correlations for estimating the residual undrained shear strength of liquefied soils in dam foundations." *Proceedings of 5th International Conference on Recent Advances in Geotechnical Earthquake Engineering and Soil Dynamics and Symposium in Honor of Professor I.M. Idriss* (CD-ROM), University of Missouri at Rolla, Missouri.

Isenhower, W.M. and Wang, S.T. (2013). *Technical Manual for LPILE 2013*, ENSOFT, Inc., Austin, Texas, USA.

Ishihara, K. and Cubrinovski, M. (2004). "Case studies on pile foundations undergoing lateral spreading in liquefied deposits." *Proceedings of the 5th International Conference on Case Histories in Geotechnical Engineering*, New York, Paper No. 5.

Japan Road Association (JRA) (1990). *Specification for Highway*

Bridges, Part V, Seismic Design, JRA, Japan.

Kulhawy, F. H. and Mayne, P. W. (1990). *Manual on Estimating Soil Properties for Foundation Design*, EL-6800, Research Project 1493-6, Electric Power Research Institute, Palo Alto, California.

Kutter, B.L. and Wilson, D.W. (1999). "De-liquefaction shock waves." *Proceedings of the 7th U.S.-Japan Workshop on Earthquake Resistant Design of Lifeline Facilities and Countermeasures Against Soil Liquefaction*, Seattle, 295–310.

Lin, S.S., Tseng, Y.J., Chiang, C.C., and Hung, C.L. (2005). "Damage of piles caused by laterally spreading—Back study of three cases." *Proceedings of ASCE Conferences on Seismic Performance and Simulation of Pile Foundations in Liquefied and Laterally Spreading Ground*, Davis, University of California, 121–133.

Liu, L. and Dobry, R. (1995). "Effect of liquefaction on lateral response of piles by centrifuge model tests." NCEER report to FWHA, *NCEER Bulletin*, **9**(1), 7–11.

Matlock, H. (1970). "Correlations for design of laterally-loaded piles in soft clay." *Proceedings of the 2nd Annual Offshore Technology Conference*., OTC 1204, Richardson, Texas, 577–594.

Reese, L.C., Cox, W.R., and Koop, F.D. (1974). "Analysis of laterally loaded piles in sand." *Proceedings of the 6th Annual Offshore Technology Conference*, OTC 2080, Houston, Texas, 473–483.

Rollins, K.M., Gerber, T.M., Dusty, L.J., and Ashford, S.A. (2005). "Lateral resistance of a full-scale pile group in liquefied sand." *Journal of Geotechnical and Geoenvironmental Engineering*, ASCE, **131**(1), 115–125.

Seed, R.B. and Harder, L.F. (1990). "SPT-based analysis of cyclic pore pressure generation and undrained residual strength." *Proceedings of H. Bolton Seed Memorial Symposium*, **2**, BiTech, Richmond, BC, Canada, 351–376.

Tokimatsu, K. (1999). "Performance of pile foundations in laterally spreading soils." *Proceedings of 2nd International Conference of Earthquake Geotechnical Engineering*, Seco, P.S. and Pinto, E., Eds., Balkema, Rotterdam, Netherlands, **3**, 957–964.

Tokimatsu, K. (2003). "Behavior and design of pile foundations subjected toearthquakes." *Proceedings of the 12th Asian Regional Conference on Soil Mechanics and Geotechnical Engineering*, Kuala Lumpur, Malaysia, 1065–1096.

Tokimatsu, K., Suzuki, H., and Sato, M. (2005). "Effects of inertial and kinematic interaction on seismic behavior of pile with embedded foundation." *Soil Dynamics and Earthquake Engineering*, **25**(7-10), 753–762.

Wang, S.T. and Reese, L.C. (1998). "Design of pile foundations in liquefied soils." *Proceedings of Geotechnical Earthquake Engineering and Soil Dynamics III*, Dakoulas P., Yegian, M., and Holtz R., Eds., ASCE, Reston, VA, **2**, 1331–1343.

Weaver, T.J., Ashford, S.A., and Rollins, K.M. (2005). "Response of 0.6 m cast-in-steel-sheel pile in liquefied soil under lateral loading." *Journal of Geotechnical and Geoenvironmental Engineering*, ASCE, **131**(1), 94–102.

Wilson, D.W., Boulanger, R.W., and Kutter, B.L. (2000). "Observed seismic lateral resistance of liquefying sand." *Journal of Geotechnical and Geoenvironmental Engineering*, ASCE, **126**(10), 898–906.

Wilson, D.W. (1998). "Soil-pile-superstructure interaction in liquefying sand and soft clay." Ph.D. Dissertation, University of California at Davis, California.